

Numerical Study on Wave Resistance of a High Speed Catamaran

SEUNG-HYUN KWAG

Halla University, School of Mechanical Engineering, Wonju 220-712 Korea

곽 승 현
한라대학교 기계공학부

고속 카타마란의 조파저항 수치연구

KEY WORDS: Wave Resistance 조파저항, Catamaran 카타마란, Wave Body Viscous Interaction 선체 유체상호작용, Navier-Stokes Equation 나비에스톡스 방정식, Free Surface Flows 자유표면유동

ABSTRACT: *This paper describes a numerical study to make clear the characteristics of flow fields around a high speed catamaran hull advancing on calm water. The simulation is carried out at Froude number of 0.5 with a separation to length ratios of 0.2 to 0.5. To simulate the flows, the Navier-Stokes solver is employed in which the free surface condition is included. Computations are performed in a rectangular grid system based on the Marker & Cell method. For the validation, the computation results are compared with the experiments.*

1. INTRODUCTION

Generally two types of interference resistances are known, namely, viscous interference caused by the asymmetric flow around the demihulls and its effect on the viscous flow such as boundary layer formations and the development of vortices, and wave interference resistance originated from the interaction between the wave systems of the demihulls. For high speed catamaran, velocity difference between the inner and outer side of the demihull makes the analysis of wave resistance a little difficult. Various hull forms such as hydrofoil crafts, planing boats, catamaran and surface effect ships have been developed to satisfy the design criteria, where catamaran is one of the most practical hull forms due to large deck area with small waterplane area, good transverse stability qualities and unusual resistance properties. Furthermore, there is not so many published information available for displacement catamarans at speeds

around or greater than about $F_n = 0.5$, the range specifically applicable to modern high speed displacement catamarans. Among recent experimental investigations, Insel & Molland (1991) gained the good results for wave resistance of catamaran with various separation to length ratio and Froude number. The wave resistance characteristics of catamaran, which result from the wave interference, are affected by length-displacement ratio, demihull spacing, initial trim and hull form. For high speed ships, the main subject is wave resistance.

In the present paper, the effect of wave interference was investigated and the optimum hull spacing is sought by which the wave interference can be reduced by changing the s/L . The computational results were compared with experiments.

$$\frac{\partial h_i^{n+1}}{\partial t} + (u_i + \frac{\partial u_i}{\partial z} \Delta h_i) \cdot \frac{\partial h_i^{n+1}}{\partial x} - w_i = 0 \quad (3)$$

2. NUMERICAL STRATEGY

2.1 Basic Equations and Boundary Condition

The basic equations are the Navier–Stokes and continuity equations. Pressures are obtained throughout the fluid domain by solving the Poisson equation. Iterations are automatically stopped when the pressure difference between two consecutive approximations is smaller than a certain quantity. The boundary conditions are as below. At the upstream boundary, the flow starts from zero and is accelerated up to the predefined speed. Thus, each horizontal component of velocity has the same constant value depending on the time step. The vertical component is equal to zero in each point of the upstream boundary and remains the same during the pressure computation. The pressure is static and remains the same. The bottom boundary is located far enough from the still water level. The pressure is set constant at the static value. The no-slip condition for the velocity and the Neumann condition for the pressure are applied on the body surface.

2.2 Free-Surface Movement

The free surface is moved by

$$\frac{\partial h}{\partial t} + u \frac{\partial h}{\partial x} - w = 0 \Big|_{z=0} \quad (1)$$

The boundary condition for the free-surface requires zero tangential stress and a normal stress that balances any externally applied normal stress. The displacement of the particle is given by

$$\Delta x = u \cdot \Delta t, \quad \Delta h = w \cdot \Delta t \quad (2)$$

where Δt is the time increment. On the other hand, the use of an Euler-type expression of the kinematic free-surface boundary condition makes possible to employ a higher finite difference scheme. The condition can be written as follows:

where $h = h(x, t)$ represents the elevation.

Expanding in Taylor series, the following can be obtained:

$$\frac{\partial h_i^{n+1}}{\partial t} = \frac{1}{2\Delta t} \cdot (h^{n-1} - 4h^n + 3h^{n+1}) \quad (4)$$

For the $\partial h^{n+1}/\partial x$ derivative, the third order upwind difference (TOUD hereafter),

$$c \frac{\partial h}{\partial x} = c \frac{1}{6\Delta x} (-2h_{i-3} + 9h_{i-2} - 18h_{i-1} + 11h_i) \quad (5)$$

where c is the convective velocity, can be decomposed into two parts. One is the central differencing term whose mathematical expression can be obtained by suitable Taylor expansions as follows:

$$\frac{c}{24\Delta x} (h_{i-3} - 27h_{i-2} + 27h_{i-1} - h_i) \quad (6)$$

The other is the diffusion term, which has the meaning of the fourth derivative of the velocity.

$$\frac{3c}{8\Delta x} (-h_{i-3} + 7h_{i-2} - 11h_{i-1} + 5h_i) \quad (7)$$

The latter is expected to play a role to compensate the "finiteness" of the differentiation without phase shift. Here the third derivative contributes the phase shift without damping.

$$\frac{\alpha c}{(\Delta x)^3} (-h_{i-3} + 3h_{i-2} - 3h_{i-1} + h_i) \quad (8)$$

where $\alpha = -\frac{(\Delta x)^2}{6}$ is a constant.

(8) is added to the right hand side term of (5), and the new formulation for the $\partial h/\partial x$ can be as,

$$c \frac{\partial h}{\partial x} = c \frac{1}{6\Delta x} (-h_{i-3} + 6h_{i-2} - 15h_{i-1} + 10h_i) \quad (9)$$

Introducing (4) and (9) into (3), the vertical coordinate increment at each time step can be,

$$\Delta h_i^n = \frac{3\Delta x(h_i^n - h_i^{n-1}) + \Delta t \cdot [6u_i \Delta x + u_i(\Delta h_{i-3}^n - 6\Delta h_{i-2}^n + 15\Delta h_{i-1}^n - Q_i^n)]}{9\Delta x + \Delta t \cdot [10u_i + Q_i^n \frac{\partial u}{\partial x} - 6\Delta x \frac{\partial u}{\partial z}]} \quad (10)$$

The expression is of the second order accuracy for $h(0(h^2))$ for any $u > 0$. Q_i^n in (10) is

$$Q_i^n = -h_{i-3}^n + 6h_{i-2}^n - 15h_{i-1}^n + 10h_i^n \quad (11)$$

where h at the $(n+1)^{th}$ step is calculated as

$$h^{n+1} = h^n + \Delta h^n \quad (12)$$

3. COMPUTATIONAL RESULTS

As the first example, the catamaran with Wigley demihulls was tested at Froude number of 0.5 and s/L of 0.2, 0.3 0.5. Fig. 1 shows the grid view for the Wigley-shaped catamaran. The grid is made as H-H topology to treat the free-surface movement more conveniently. The wave height contours are shown in Fig. 2. in which the s/L is changed. As the s/L becomes smaller, the divergent wave between the demihulls is eliminated and the transverse wave is dominant by the divergent wave interference. In case of s/L=0.5, the wave interference is almost disappeared and the wave pattern becomes similar to that of monohull. The effect of wave interference between the demihulls is dominant as the s/L becomes smaller and in the case of s/L=0.2, as the wave interference become larger, the effect is propagated to outer flow fields at the outer side of the demihulls. The wave resistance interference, for different s/L ratios, is given in Fig. 3, which is defined as $C_w(\text{catamaran})/ C_w(\text{monohull})$. Although the test points are not enough, the result shows that the wave interference can be effectively neglected above the particular speed which is separation dependent and indicates that higher separation results in smaller interference.

In the second example, the prototype catamaran moving at two Froude numbers of 0.45, 0.95 was numerically studied.

Fig. 4 shows the grid generation of the catamaran in which the orthogonality and minimum grid spacing are adopted. Fig. 5 shows the wave heights in which the results of monohull are compared in (a) and (b), while those of twin-hull are in (c). By the wave heights obtained, the effects of Froude number could be reviewed. The velocity vectors is shown in Fig. 6. We can see the detailed characteristics of flow pattern between the hulls of high speed catamaran.

4. CONCLUSION

The flow characteristics for the high speed catamaran is numerically investigated comparing the wave profiles with the results of Wigley's and displacement catamaran. The effect of wave interference was reviewed and the optimum hull spacing is sought by which the wave interference can be reduced by changing the s/L. The results between computation and experiment were compared each other for the validation of the present numerical codes. In the future, the computation should be continued over a wide range of Froude numbers because they are of great value for the initial design of high speed catamaran.

REFERENCES

- Insel, H. and Molland, A. F. (1991), "An Investigation into the Resistance of High Speed Displacement Catamarans", Trans, RINA

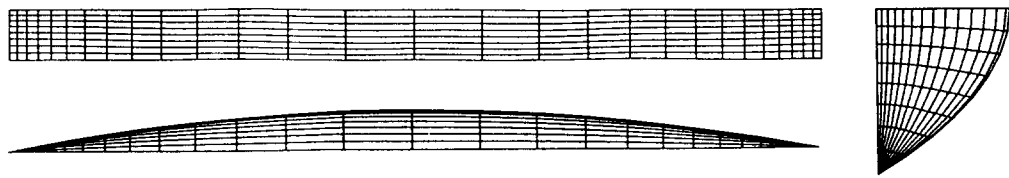


Fig. 1 Grid view for Wigley-shaped catamaran

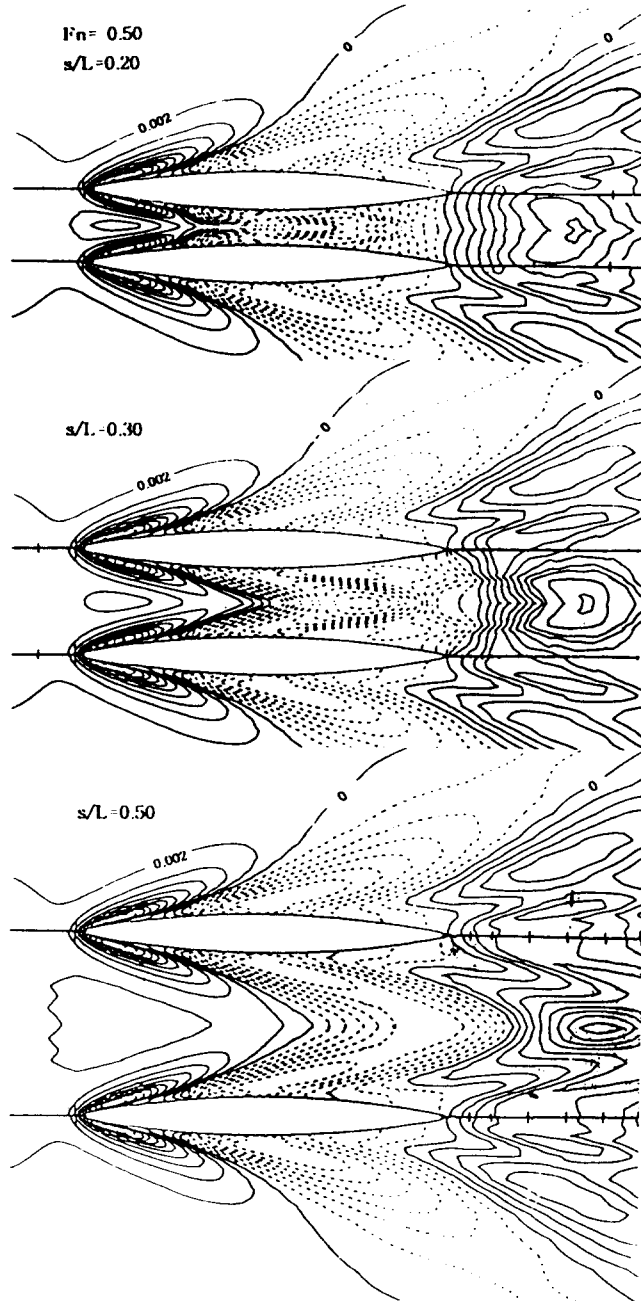


Fig. 2
Wave height contour
at $F_n=0.50$ ($s/L=0.20,$
 $0.30, 0.50$)

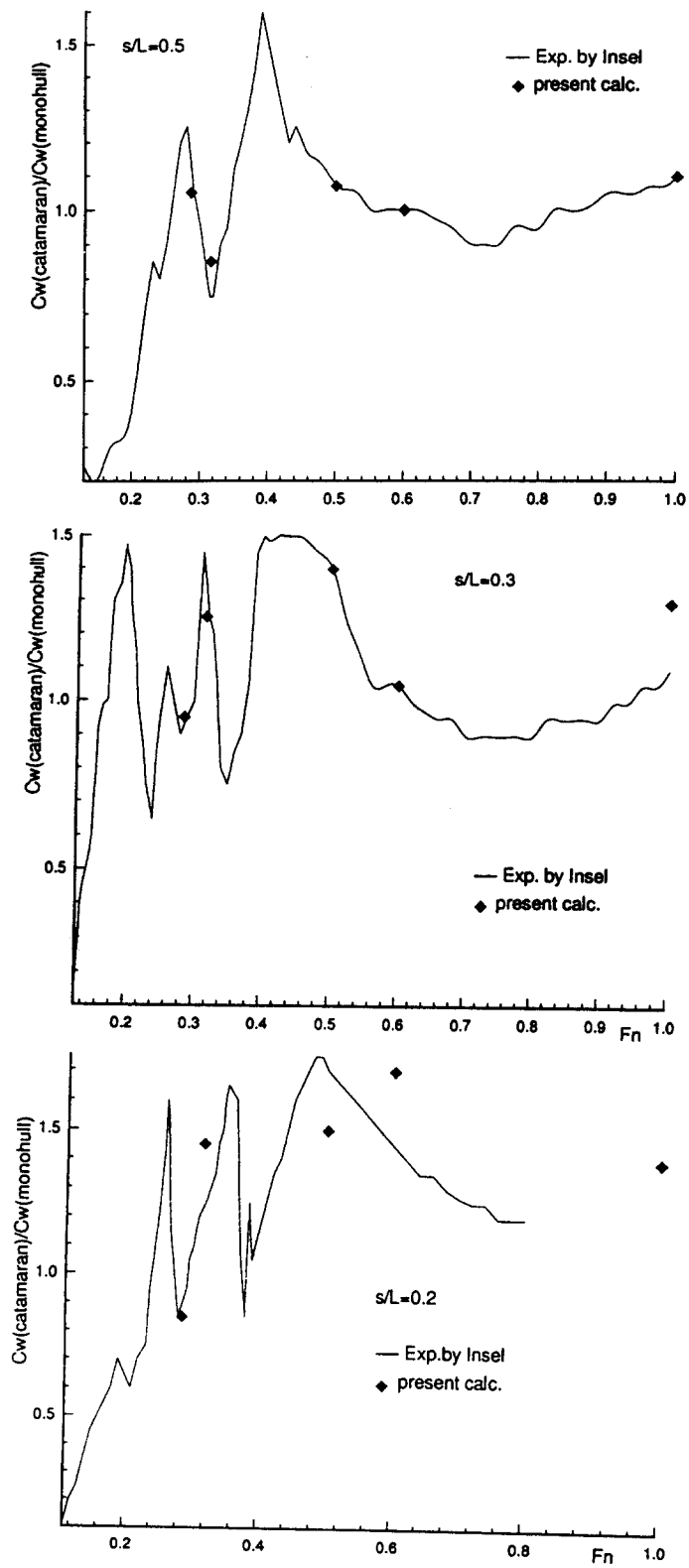


Fig. 3 Wave resistance interference

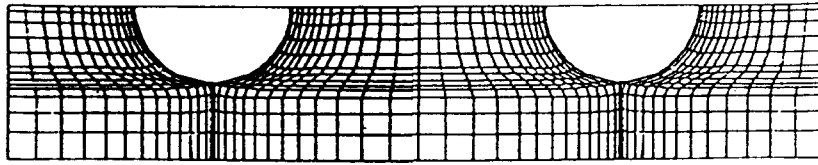


Fig. 4 Grid generation for catamaran

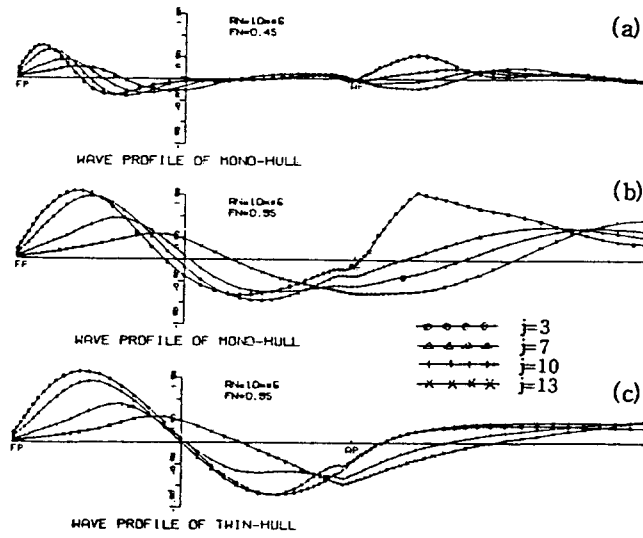


Fig. 5 Wave height comparison for mono and twin hull

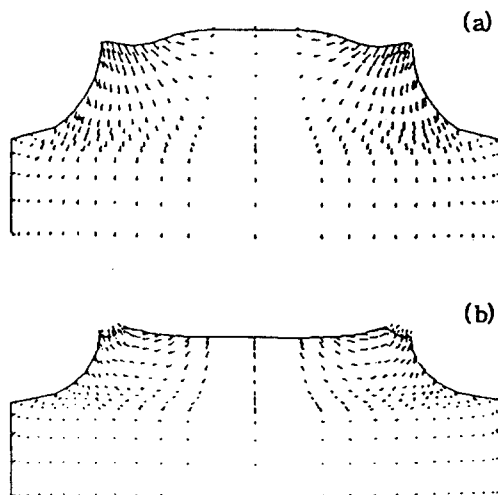


Fig. 6 Velocity vectors for catamaran
(a) $x/L=0.55$ (b) $x/L=0.90$